

Characteristics and classification of A-type supergiants in the Small Magellanic Cloud

Christopher J. Evans^{1*} and Ian D. Howarth^{2†}

¹*Isaac Newton Group of Telescopes, Apartado de Correos 321, 38700 Santa Cruz de La Palma, Canary Islands, Spain*

²*Department of Physics and Astronomy, University College London, Gower Street, London WC1E 6BT, UK.*

Dates to be inserted

ABSTRACT

We address the relationship between spectral type and physical properties for A-type supergiants in the SMC. We first construct a self-consistent classification scheme for A supergiants, employing the calcium K to $H\epsilon$ line ratio as a temperature-sequence discriminant. Following the precepts of the ‘MK process’, the same morphological criteria are applied to Galactic and SMC spectra with the understanding there may not be a correspondence in physical properties between spectral counterparts in different environments. We then discuss the temperature scale, concluding that A supergiants in the SMC are systematically cooler than their Galactic counterparts at the same spectral type, by up to $\sim 10\%$. Considering the relative line strengths of $H\gamma$ and the CH G -band we extend our study to F and early G-type supergiants, for which similar effects are found. We note the implications for analyses of extragalactic luminous supergiants, for the flux-weighted gravity-luminosity relationship and for population synthesis studies in unresolved stellar systems.

Key words: Galaxies: individual: Magellanic Clouds – stars: fundamental parameters – stars: early-type

1 INTRODUCTION

A-type supergiants are important probes of metallicity in nearby galaxies (e.g., McCarthy et al. 1995; Venn et al. 2000; Bresolin et al. 2002). This is because of their intrinsic luminosity and relatively small bolometric corrections (ensuring that they are among the visually brightest stars in any galaxy; e.g., Humphreys 1983), and their spatial isolation (which contrasts with O- and B-type stars, which are frequently found in clusters or associations, or in binary systems with companions of comparable brightness). Moreover, not only are the optical spectra of A-type supergiants typically free of significant contamination from spatially unresolved companions, but they also exhibit lines from a relatively wide range of elements, which can be modeled reasonably satisfactorily using relatively simple LTE atmospheres (cf. Venn 1995).

A-type stars can also be important – occasionally dominant – contributors to the integrated light of more distant, unresolved galactic systems (e.g., Brotherton et al. 1999). In the interpretation of such unresolved systems, as well as the spectra of individual stars, the correspondence between spectral morphology and fundamental stellar parameters is

a key issue. We address this issue in the present paper, motivated by the need to classify the A-type stars observed in our forthcoming 2dF survey of the luminous-star content of the SMC (Evans et al. 2003), and to assign consistent and accurate effective temperatures to them.

2 SPECTRAL CLASSIFICATION: PRINCIPLES

By way of introduction to the philosophy of spectral classification which we adopt, we can do no better than draw on the discussion given by Morgan (1937) in his seminal paper on the classification of A–K-type spectra:

“There would be a number of advantages in having a two-dimensional empirical spectral classification; the operations of the determination of actual values of stellar temperatures and luminosities could then be separate from the problem of classifying spectra. Suppose that it had been the custom to publish the actual effective temperature instead of the empirical spectral type. . . the classification, then, would be subject to two sources of error: (1) the error inherent in the criteria themselves and the observational error introduced in their estimation or measurement; and (2) the error introduced in the reduction of the observational data to a temperature scale. The uncertainties introduced in (2) increase unnecessarily the uncertainty in the actual operation of classification.”

* email: cje@ing.iac.es

† idh@star.ucl.ac.uk

Thus, to quote a more recent doyen of classification,

“One of the basic underlying principles of the MK approach to spectral classification has been the preservation of its independence from theoretical or other external information, with regard to both the systemic formulation and its practical application”

(Walborn 1979). We stress this independence here because it contrasts with the practice of some analysts who infer ‘spectral types’ from model-atmosphere analyses (e.g., in the context of SMC A-type supergiants, Venn 1999).

Spectral classification, according to the precepts of the ‘MK Process’, therefore follows observed spectroscopic characteristics, not inferred physical properties. A corollary of this is that two stars with the same spectral types according to the traditional two-parameter MK scheme may have different physical properties if they differ in a third parameter, such as metallicity. We investigate the extent of these differences, insofar as they apply to the SMC, in the latter part of this paper.

3 OBSERVATIONS

If the MK philosophy is to be extended to galaxies beyond the Milky Way, then the spectral morphology of an A0 star in the SMC, for example, *should* resemble that of an A0 star in the Galaxy, in so far as the projection of a multi-dimensional parameter space onto a two-dimensional classification scheme allows; Lennon (1997) provides an exemplary illustration of this principle in his discussion of SMC B-supergiant spectra. Thus, notwithstanding the well-established differences in metallicity between SMC and Galactic stars, it is necessary to use Galactic standards as a starting point.

3.1 Galactic standards

We found rather few suitable digital spectra of A-type classification standards in the literature, and so resorted to obtaining our own; to ensure continuity at the extremes of the A-star sequence, we also observed a handful of late-B and early-F stars. Details of the targets are given in Table 1.

The first set of spectra was obtained in 2000 July, during the course of another programme, using the 2.5-m Isaac Newton Telescope (INT) with the Intermediate Dispersion Spectrograph (IDS). A 400B grating, 500-mm camera, and $1024 \times 1024 \times 24 \mu\text{m}^2$ Tektronix detector (windowed to 300 pixels in the spatial direction) gave wavelength coverage of approximately $\lambda 3700\text{--}4900\text{\AA}$ at $R \simeq 1900$ (as determined from arc-lamp exposures).

Further observations were obtained with the 4.2-m William Herschel Telescope (WHT) in 2001 August, again during another programme, using the Intermediate-dispersion Spectroscopic and Imaging System (ISIS) with 600B and 1200B gratings (according to the requirements of the principal programme) with a $4096 \times 2048 \times 13.5 \mu\text{m}^2$ EEV12 CCD (windowed to 700 pixels in the spatial direction and binned by a factor of two in the dispersion direction). The wavelength range from the 600B grating was $\lambda 3750\text{--}5400\text{\AA}$ at $R \simeq 2900$; coverage with the 1200B grating was $\lambda 3910\text{--}4780\text{\AA}$ at $R \simeq 5800$. To provide a more uniform dataset, the WHT A-star spectra were smoothed to

$R \simeq 1600$, to match the 2dF data, for classification and measurement purposes.

The data typically have signal-to-noise ratios (s:n) $\gtrsim 200$ per wavelength bin. Sample spectra are shown in Figure 1.

3.2 SMC data

As mentioned previously, the initial motivation for the present work was the need to classify and interpret, in a systematic and consistent manner, the A-star spectra obtained in our 2dF survey of the population of luminous blue stars in the SMC. The great bulk of our SMC dataset therefore comes from this source, with observations obtained in 1998 September and 1999 September.

2dF is a fibre-fed, multi-object dual spectrograph mounted at the AAT (Lewis et al. 2002). We used the system with 1200B gratings, giving wavelength coverage of $\sim 3900\text{--}4700$ at $R \simeq 1600$. The s:n varies between $\sim 15\text{--}150$ for the spectra retained for analysis, averaging ~ 25 .

Because of initial concerns with the reliability of background subtractions in the 2dF data, we obtained supplementary spectra of \sim two dozen representative A-type SMC stars in traditional long-slit mode in 2001 July, using the AAT’s RGO spectrograph with a 1200B grating and EEV CCD ($R \simeq 2700$). The observations have a useful wavelength range of $\sim 3700\text{--}5500\text{\AA}$, with s:n $\sim 50\text{--}100$. They demonstrate that there are, in fact, no systematic problems with the 2dF data.

Illustrative 2dF SMC spectra are shown in Figure 2.

4 SPECTRAL CLASSIFICATION: PRACTICE

4.1 Luminosity classification

We begin our discussion by emphasising the distinction between luminosity (intrinsic brightness) and luminosity *class* (characterising the appearance of the spectrum). Luminosity classes were allocated in our SMC work using the Azzopardi (1987) calibration between luminosity class and $H\gamma$ equivalent width; mean values for the spectral types considered here are given in Table 2. Azzopardi’s study was, necessarily, based on limited data (low-dispersion, objective-prism photographic spectra acquired in the 1970s) and unfortunately the superior observational material of Balona & Crampton (1974) does not extend beyond the earliest A-subtypes. We intend to revisit the relationships between $H\gamma$ line strength, luminosity class, absolute magnitude, and metallicity in due course. This is not necessary in the present, morphologically-based, work, but attention is drawn to the discussion in section 5.5.

The A-star spectra in Fig 2 all have greater $H\gamma$ equivalent widths than those for the Azzopardi Ib calibration. They are also smaller than one would expect for class III spectra (e.g. Balona & Crampton 1974), and have therefore been assigned class II here. In the absence of similar calibrations beyond A7, the two F-type spectra are classified by extrapolation, as luminosity class I.

Table 1. Galactic targets. Sources of spectral types are (in decreasing order of preference): M73, (Morgan & Keenan 1973); M43, (Morgan et al. 1943); M55, (Morgan et al. 1955); M53, (Morgan et al. 1953); M50, (Morgan & Roman 1950); S54, (Slettebak 1954); GG7, (Gray & Garrison 1987); GG9, (Gray & Garrison 1989); G01, (Gray et al. 2001); A81, (Abt 1981); A85, (Abt 1985); C69, (Cowley et al. 1969). The photometric data in columns 6 & 7 are taken from the The General Catalogue of Photometric Data (Mermilliod et al. 1997), and are used with intrinsic colours from Fitzgerald (1970) to derive the estimated reddening values given in column 8, where we retain unphysical negative values for statistical purposes. Where available, column 9 contains $v_e \sin i$ values (in km s^{-1}) from Abt & Morrell (1995). ‘Tel.’ identifies the telescope, and, in the case of WHT observations, the grating (600B or 1200B). The final column is the ratio of the measured depth of the Ca *K* line to that of the Ca *H* + He blend.

HD	Name	Sp. Type	Source	<i>V</i>	(<i>B</i> – <i>V</i>)	<i>E</i> (<i>B</i> – <i>V</i>)	$v_e \sin i$	Tel.	$\frac{1-I_K}{1-I_{(H+He)_q}}$
432	$\beta/11$ Cas	F2 III–IV	M73	2.27	0.34	–0.03	–	INT	1.01
571	22 And	F0 II	M50	5.04	0.40	0.18	–	INT	1.04
1404	$\sigma/25$ And	A2 V	GG7	4.52	0.06	0.01	110	INT	0.51
3283		A3 II	GG9	5.79	0.28	0.21	100	INT	0.74
3940	V755 Cas	A1 Ia	M55	7.27	0.72	0.69	–	INT	0.46
6130		F0 II	M73	5.92	0.49	0.27	23	INT	0.95
7927A	$\phi/34$ Cas	F0 Ia	M55	4.99	0.68	0.53	23	INT	1.00
8538	$\delta/37$ Cas	A5 V	M53	2.68	0.13	–0.02	110	INT	0.77
10845	VY Psc	A8 III	GG9	6.58	0.25	–0.01	85	INT	0.94
12216	50 Cas	A1 V	S54	3.96	–0.01	–0.03	85	INT	0.39
12279	52 Cas	A0 V	GG7	5.99	0.03	0.04	255	INT	0.30
12953	V472 Per	A1 Ia	M55	5.69	0.62	0.59	30	W06	0.63
13041	58 And	A4 V	GG9	4.82	0.12	0.00	120	INT	0.74
13476		A3 Iab	M55	6.44	0.60	0.54	20	INT	0.56
14489	$\iota/9/V474$ Per	A2 Ia	M55	5.18	0.37	0.32	25	INT	0.46
15316		A3 Iab	M55	7.23	0.77	0.71	–	W06	0.67
17378	V480 Per	A5 Ia	M55	6.25	0.89	0.79	25	W06	0.82
20902		F5 Ib	M73	1.79	0.48	0.22	–	INT	1.02
148743		A7 Ib	G01	6.49	0.37	0.24	43	W12	0.95
161695		A0 Ib	C69	6.24	0.00	0.00	25	W12	0.27
172167	$\alpha/3$ Lyr	A0 V	M73	0.03	0.00	0.01	15	INT	0.22
173880	111 Her	A3 V	GG9	4.36	0.13	0.05	70	W12	0.77
186155		F5 II	M73	5.07	0.39	0.01	–	INT	1.02
187983		A1 Iab	M55	5.58	0.69	0.66	45	W12	0.49
192514	30 Cyg	A3 III var	S54	4.82	0.10	0.01	160	INT	0.68
195324	42 Cyg	A1 Ib	C69	5.88	0.52	0.50	15	INT	0.34
196379		A9 II	M73	6.13	0.40	0.22	21	INT	0.95
197345	$\alpha/50$ Cyg	A2 Ia	M73	1.24	0.10	0.05	30	INT	0.51
203280	$\alpha/5$ Cep	A7 IV–V	M53	2.46	0.22	0.00	180	INT	0.87
205835	74 Cyg	A5 V	GG9	5.04	0.17	0.02	185	INT	0.82
207260	$\nu/10$ Cep	A2 Ia var	M55	4.29	0.52	0.47	40	INT	0.46
207673		A2 Ib	M55	6.47	0.41	0.36	35	INT	0.37
210221	V399 Lac	A3 Ib	M55	6.14	0.42	0.36	20	INT	0.65
211336	$\epsilon/23$ Cep	F0 V	M43	4.19	0.28	–0.04	80	INT	0.96
212593	4 Lac	B9 Iab	M50	4.57	0.09	0.09	–	INT	0.32
213558	$\alpha/7$ Lac	A2 V	S54	3.76	0.02	–0.03	115	INT	0.37
213973		A9 III	A81	6.01	0.32	0.04	–	W06	0.99
216701	1 Psc	A7 IV	GG9	6.11	0.20	–0.02	80	W06	0.93
222275		A5 III	A85	6.59	0.55	0.40	–	INT	0.80
223385	6/V566 Cas	A3 Ia	M55	5.44	0.67	0.61	30	W06	0.76

HD12953: In contrast with the other Galactic standards, the observed *K*/*H* ϵ ratio for this star is in relatively poor accord with its MK spectral type (see Figure 4); from the criteria adopted here, HD 12953 would be classified as A3 – with the exception of slightly weaker metal lines and a smaller Ca *K* intensity, its spectrum is similar to that of HD 223385 (classified by M55 as A3 Ia). However, 12953’s A1 Ia spectral type carries the authority of a Morgan et al. (1955) classification. The cause of this discrepancy is not clear.

A note on ‘HD 187982’: The HD catalogue assigns BD+24 3914 two numbers (HDs 187982 and 187983), and two spectral types (F5 and A2, respectively), noting that ‘the spectrum is composite’. Humphreys (1978), Abt & Morrell (1995), and others, have subsequently identified the A-type star with HD 187982. In her study of spectroscopic binaries, Hendry (1981), also referring to HD 187982, concluded that there is ‘no trace of a composite spectrum’, on the basis of greatly superior spectroscopic material, and she mentions work by McAlister (1979) in which the star was unresolved using speckle interferometry with the Kitt Peak 4-m telescope.

It is important to note that the compilers of the HD catalogue habitually assigned two numbers to what they considered to be single, composite-spectra systems. However, in this case it appears almost certain that HD 187982 is non-existent, and that the A-type supergiant BD+24 3914 should be identified with HD 187983 alone.

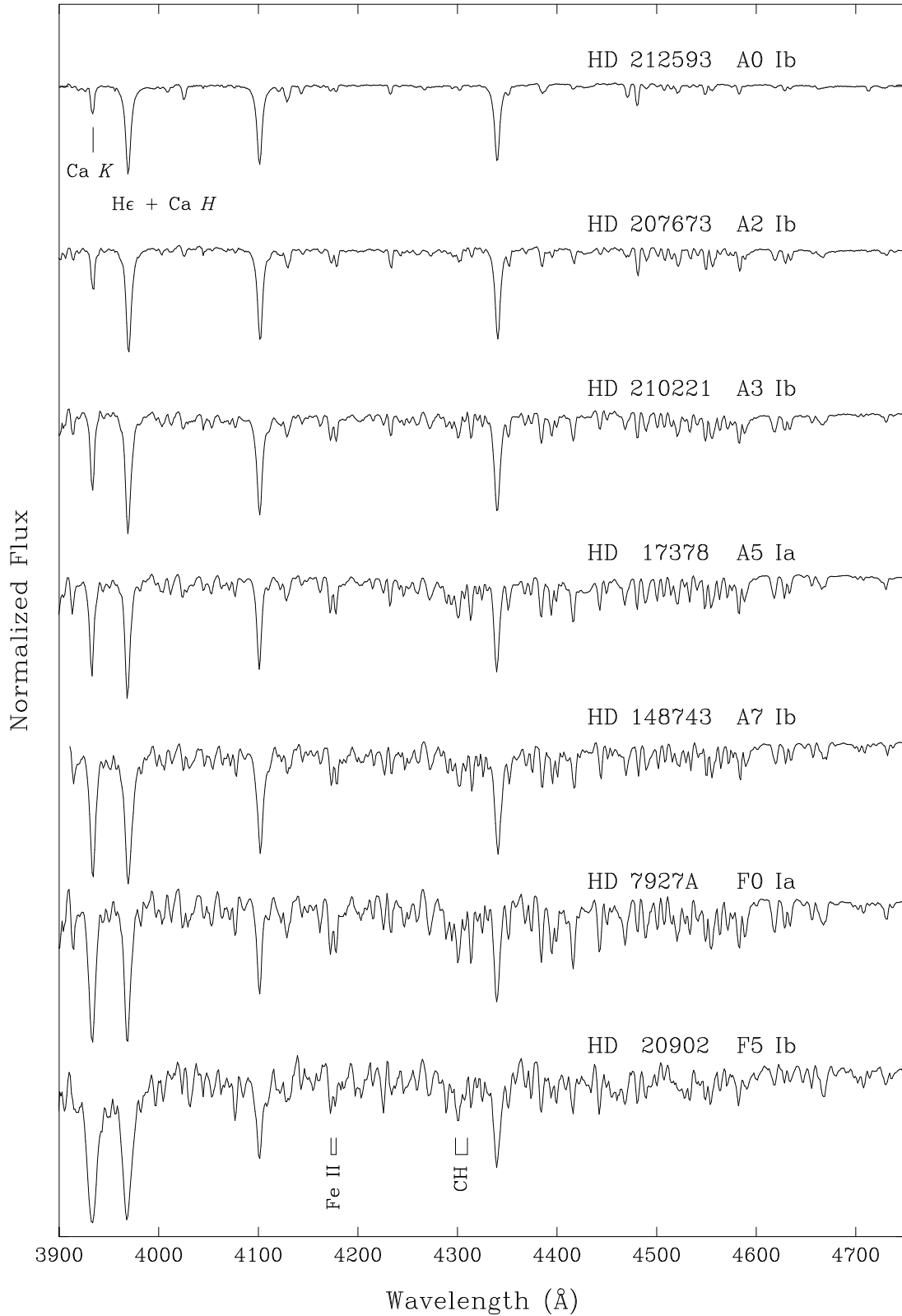


Figure 1. Spectra of Galactic A- and early-F-type stars. Identified features are Ca II *K* $\lambda 3933$; the Ca II *H* $\lambda 3969$ + He blend; Fe II $\lambda 4173-78$; and the CH *G*-band, $\sim \lambda 4300$. Successive spectra are offset by one continuum unit.

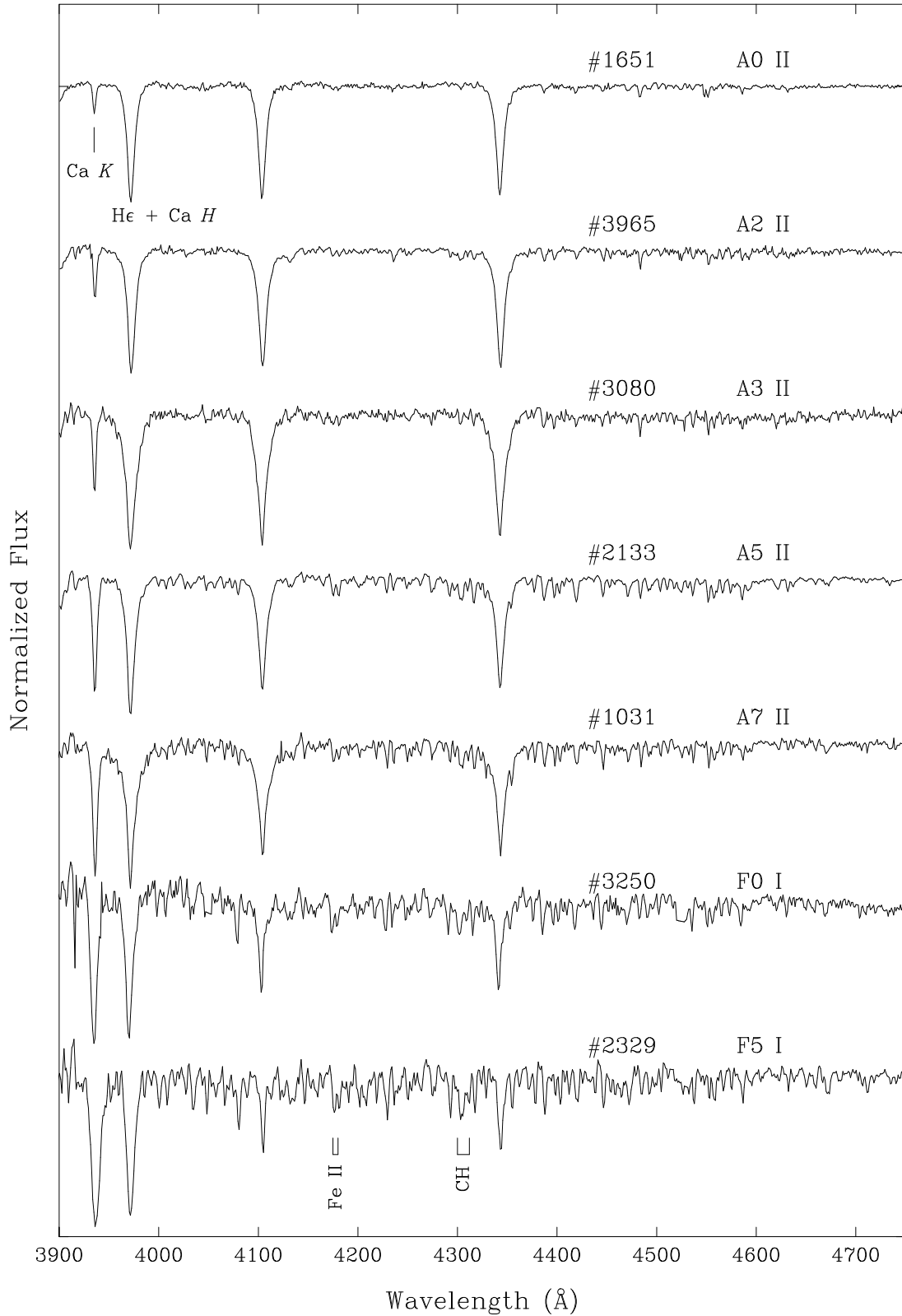


Figure 2. 2dF spectra of representative A- and early F-type supergiants in the SMC, identified by serial number in our forthcoming 2dF spectroscopic catalogue. Precise radial velocity measurements are not possible from the 2dF data so the spectra are shown here have not been corrected to the stellar rest frame. The stars have been classified using the criteria in Table 3.

Table 2. Mean H γ equivalent width calibration for the MK ‘dagger’ spectral types used in the current work, from Azzopardi (1987).

Sp. Type	Ia	Iab	Ib
A0	2.35	3.15	4.20
A2	2.60	3.40	4.70
A5	3.00	4.00	5.70
A7	3.35	4.55	6.55

4.2 Temperature classification of A-type stars

The foundations of modern spectral classification, elaborated by Morgan et al. (1943), were largely in place by the time Annie Cannon produced the Henry Draper Catalogue (Cannon & Pickering 1924), following earlier work by Fleming, Maury and others (Pickering 1890; Maury 1897), in part under Pickering’s supervision. In the A-type domain, Cannon’s main classification criterion was the intensity of the Ca K line ($\lambda 3933\text{\AA}$) with respect to H δ and the blend of He + Ca H ($\lambda 3968\text{\AA}$). Morgan (1937) also identified the Ca II K line as a useful diagnostic feature; it is the most conspicuous discriminant of temperature for A-type stars.

We therefore investigated the use of the K line and the He/Ca H blend as a temperature discriminant. Although there are, potentially, problems with the use of the K line (discussed in Section 4.3), it has the advantage that a spectrum can be quickly and accurately classified, even at low signal-to-noise. While other classification criteria exist, such as the ratio of Ca I $\lambda 4226$ to Mg II $\lambda 4481$ (Yamashita et al. 1977), the weakness of most metal-line features in the spectra of (metal-deficient) SMC stars makes them less useful for our purposes, especially in view of the modest s:n in the majority of our 2dF spectra.

4.2.1 Galactic stars

The ratios of measured $K/\text{He}(\text{+}H)$ line depths in the Galactic stars are given in Table 1, and are shown in Figure 4 as a function of spectral type;¹ as expected, there is a well-defined sequence. However, there is some overlap (e.g., between A1 and A2). In view of this, and the relatively poor s:n of the SMC data, we adopt a slightly less fine classification unit, using only the ‘dagger’ subtypes for which standards are advanced by Morgan & Keenan (1973); the results are summarised in Table 3, which affords an almost completely ‘clean’ segregation of the Galactic standards (Fig. 4).

4.2.2 SMC stars

The criteria in Table 3 have been adopted for classifying the SMC stars. Even for quite poor-quality data, the K/He

¹ In principle, the measured line-depth ratio may be influenced by spectral resolution; in practice, we circumvent this problem by convolving all our spectra to the resolution of the 2dF data. The equivalent-width ratio, which should be independent of resolution, proved to be a less sensitive and consistent discriminant in practice.

Table 3. Classification bins for A-type classifications, derived from observations of Galactic targets, using the system of Morgan et al. (1943).

Ca K / He + Ca H	Spectral Type
<0.33	A0
0.33–0.53	A2
0.53–0.75	A3
0.75–0.85	A5
0.85–0.95	A7
>0.95	A9, F0 or later

ratio can be measured to better than ~ 0.05 , which is generally sufficient for classifications uncertain to better than one subtype at our adopted classification resolution.

The scheme in Table 3 is largely in accord with the original criteria of Cannon & Pickering. The sensitivity of K/He to spectral type falls off towards cooler temperatures, and for both A9 and F0 types the K line is very strong ($K/\text{He} \simeq 1$); these subtypes are essentially indistinguishable in the 2dF data, and we grouped them under the ‘F0’ label. (Still later spectral types are discussed in section 4.4)

The distinction between A5 and A7 is relatively subtle, but is achieved consistently. This is illustrated by the signal-weighted mean spectra at each spectral subtype shown in Fig. 3. The smooth progression of weak metal features with spectral type (e.g. Fe II $\lambda\lambda 4173\text{--}78$) demonstrates that the classifications are at least internally consistent, while discrimination at A3/A5/A7 is confirmed by the reversal of the $K/\text{H}\delta$ ratio between these subtypes.

4.3 Classification caveats

Although relatively quick and simple to use, the Ca K (and H) lines are not without concerns for classification purposes.

4.3.1 Luminosity effects

Gray & Garrison (1989) noted that using the calcium/hydrogen ratio may introduce effects into the spectral-type classifications because the Balmer lines are sensitive to luminosity. However, the measurements in Table 1 show no obvious trend with luminosity class, as is illustrated by in Fig. 4. Although the sampling is insufficiently dense to rule out small differences between classes on average, the dispersion at a given spectral subtype is evidently much larger than such differences. In any case, our 2dF sample is overwhelmingly dominated by high-luminosity objects.

4.3.2 Interstellar contamination

It has been known for a century that Ca II H & K absorption lines arise in the interstellar medium (Hartmann 1904). The interstellar lines are not distinguishable in intermediate-dispersion spectra, and could therefore introduce a bias into the spectral classifications. (Although dust extinction towards SMC stars is generally rather small, with $E(B - V) \lesssim 0.1$, the velocity dispersion in the line-of-sight interstellar material enhances the effect of resonance-line absorption.)

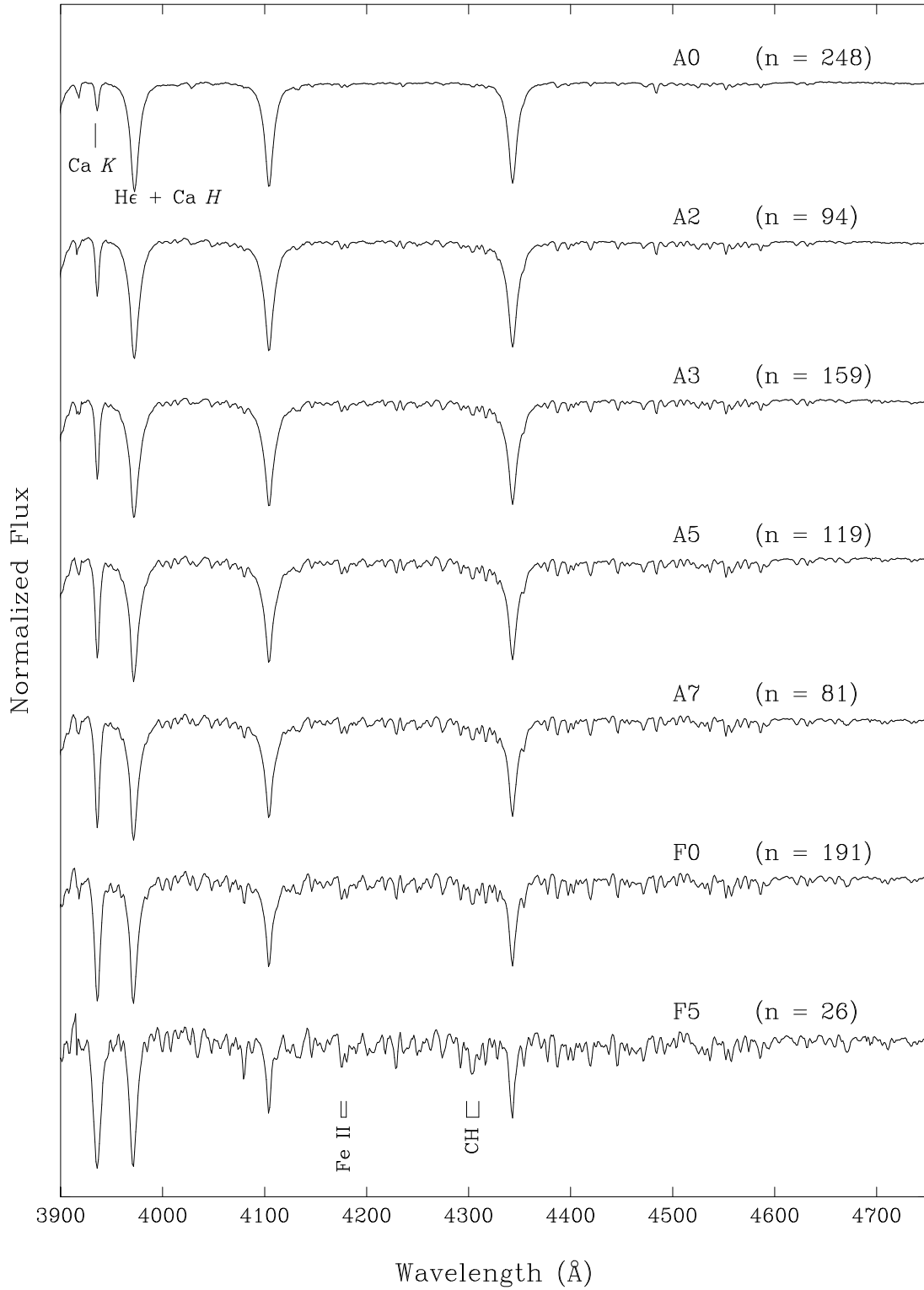


Figure 3. Means of 2dF spectra for AF stars in the SMC. The numbers of individual spectra contributing to the means are given in parentheses.

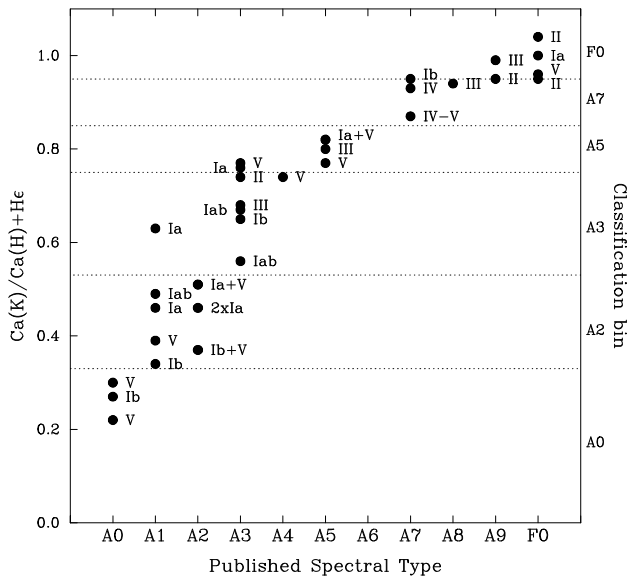


Figure 4. Ratio of core depth of Ca K to Ca $H + He$, as a function of spectral type, for the sample of Galactic A-type spectra listed in Table 1. Note that there is no obvious luminosity-class dependence of the ratio. Dashed lines show the adopted classification boxes. The most discrepant point, at A1 Ia, is HD 12953, discussed in Table 1.

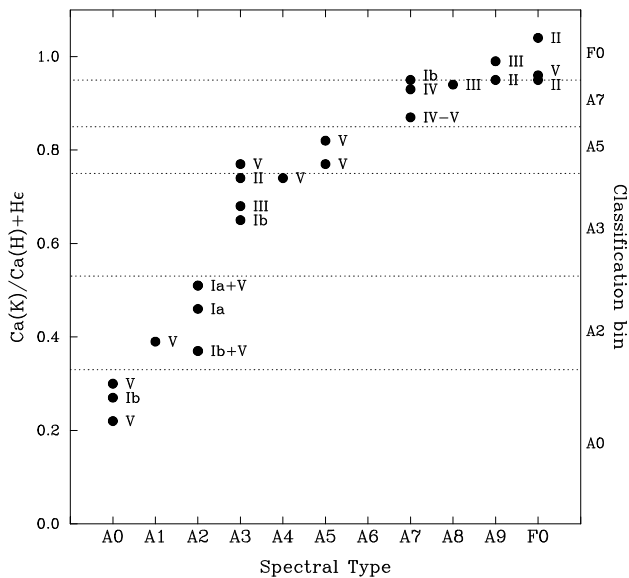


Figure 5. As in Figure 4 except that only stars with values of $E(B - V) < 0.40$ are shown.

To assess the likely impact of any contamination, reddening values were calculated as a crude surrogate for interstellar-line equivalent widths of Galactic targets (Table 1). Reassuringly, there is no evidence of segregation between high- and low-reddening targets (cf. Fig. 5). This is consistent with our expectations that (i) interstellar absorption is a relatively small contributor to the total H, K equivalent widths for A-type stars, and (ii) interstellar H and K

will vary in tandem, so that they have only a second-order effect on the $K/(He + H)$ ratio.

4.3.3 Metallicity effects

One of the most important considerations when using the calcium line as a classification criterion is the reduced metallicity of the SMC. One approach to the metallicity issue is given in Venn (1999), where the spectral types of a sample of SMC A-type supergiants were adjusted in the light of model-atmosphere analysis. Our approach to the issues regarding classification that arise from this and other studies were discussed in Section 2. In the current context of classifying the 2dF sample, the criteria in Table 3 are applied on the basis that they are the *morphological* counterparts of Galactic criteria, with the explicit understanding there may not be a correspondence in *physical* properties between Galactic and SMC stars.

4.3.4 Rotational broadening effects

The influence of rotational broadening on A-stars classification has been discussed by Gray & Garrison (1987). They defined low and high $v_e \sin i$ standards on the basis that broadening of the K line in rapid rotators may affect the classification process. Gray & Garrison (1989) subsequently concluded that at type A5 and later this effect is reduced, such that the Ca K/He ratio can be safely used for rapid rotators.

This is not of direct concern in the 2dF dataset because of the distance (i.e., luminosity) selection effect. Typical rotational velocities for A-type supergiants are low (of order $20\text{--}30 \text{ km s}^{-1}$; e.g., Abt & Morrell 1995; Venn 1995), so rotation is not a significant issue. For comparison, the “high” $v_e \sin i$ stars referred to by Gray & Garrison (1987) have velocities in the range of $150\text{--}275 \text{ km s}^{-1}$ (with luminosity types ranging from III to V).

In principle there could be a systematic difference in the rotational velocity distributions between the Galaxy and the SMC, as discussed by Maeder et al. (1999) in reference to B-type stars. Rotation could also have an indirect effect through the Galactic stars used here to describe the classification framework. Where available, rotational velocities from Abt & Morrell (1995) are given in Table 1 for our Galactic targets. The majority of the Galactic stars have relatively low velocities, and those with faster rotation are not particularly discrepant in Figure 4, suggesting that rotational effects are unlikely to play a significant rôle in the current work.

4.4 Spectral classification of F- and later-type stars

The K/He ratio is useful for distinguishing between A spectral subtypes, even in data of moderate to poor quality, but is not a sufficient criterion to distinguish late-B from early-A, nor early-F from late-A stars.

The B stars are straightforwardly identified by the presence of helium lines (e.g. Lennon 1997), while the ~ 100 supergiants with spectral types later than F0 observed in the 2dF sample (as a result of photometric errors in the

Table 4. Classification bins for F & G-type classifications, derived from Jaschek & Jaschek (1990).

Spectral Type	Criteria
F0–F2	Ca <i>K</i> / He + Ca <i>H</i> ~ 1
F5	Clear presence of CH <i>G</i> -band
F8	<i>G</i> -band / H γ = 0.5–0.75
G0	<i>G</i> -band / H γ = 0.75–0.9
G2	<i>G</i> -band \sim H γ ; H γ > Fe I $\lambda 4325$
G5	H γ \sim Fe I $\lambda 4325$
G8	H γ < Fe I $\lambda 4325$

input catalogue) were classified using the INT data as a point of reference, in combination with the criteria given by Jaschek & Jaschek (1990). Essentially, F-type stars are characterized by increasingly strong metal lines (visible even at SMC metallicity); this behaviour is most obvious in the ratio of Ca *K* to H γ , but is clear in other features, such as the $\lambda 4300$ *G*-band. The adopted ‘late-type’ classification scheme, which takes into account the characteristics of the 2dF dataset (low s:n, weak metal lines), is summarised in Table 4.

5 THE TEMPERATURES OF A-TYPE SUPERGIANTS IN THE SMC

For population syntheses, IMF modelling, and many other circumstances where quantitative analyses of individual stars is infeasible, it is important to have an accurate ‘look-up table’ of correspondences between physical and morphological characteristics. In the remainder of this paper, we examine this issue in the light of our remarks in section 2, with particular emphasis on the temperature scale for A-type stars.

5.1 Model atmospheres

The model-atmosphere structures used here are ATLAS9 models (Kurucz 1991), calculated by Collaborative Computational Project #7 (CCP7; <http://ccp7.dur.ac.uk/>). The models assume plane-parallel geometry, hydrostatic equilibrium, and LTE, and include the effects of line blanketing. The majority of the A-type stars in the 2dF sample are of luminosity types of Ib or II, where LTE has been shown to be a reasonable approximation (e.g. Pryzbilla 2002). Departures from LTE become increasingly important in type Ia supergiants; however, in the current context, the ATLAS9 models have the advantage that results can be achieved quickly, relatively simply, and that they include the important effects of line blanketing.

The low-metallicity CCP7 models that we used incorporate a microturbulent velocity, ξ , of 2 km s⁻¹. This is just below the range of $\xi = 3\text{--}8$ km s⁻¹ found in Venn’s A-supergiant analyses (Venn 1995, 1999), although many of her targets yielded values in the 3–4 km s⁻¹ range. Spectra synthesized using 2- and 4-km s⁻¹, solar-abundance models are essentially identical, and differences resulting from use of an 8-km s⁻¹ grid are negligible. We conclude that the CCP7 models are adequate for the current investigation.

Hubeny’s unpublished SYNPEC43 code was used for the spectral synthesis, running under the IDL SYNPLLOT wrapper (also written by Hubeny). The necessary atomic and molecular line-lists were downloaded from the TLUSTY web page.² Both Rayleigh-scattering and H⁻-ion opacities were included in the calculations.

The synthetic spectra were convolved with typical $v_e \sin i$ values (~ 30 km s⁻¹), and smoothed to a resolution comparable to that of the 2dF data. In all cases, instrumental broadening dominates.

5.2 Model grid

Three main spectral regions were investigated:

- $\lambda 3900\text{--}4050\text{\AA}$: Ca *K*/He ϵ (important in A-types).
- $\lambda 4250\text{--}4450\text{\AA}$: CH *G*-band/H γ (F and G-types).
- $\lambda 4450\text{--}4540\text{\AA}$: He I $\lambda 4471$ /Mg II $\lambda 4481$ (late-B stars).

The atomic species included for the spectral-synthesis investigation of B and A-types were H, He, C, N, O, Mg, Si and Ca. For the later types, in addition to the molecular line-list, Mn, Cr and Fe were included.

SYNPLLOT was used to generate synthetic spectra on a small grid covering appropriate values of temperature and gravity. The temperature range of the grid was chosen by reference to Schmidt-Kaler (1982). Only approximate values are required for the $\log_{10} g$ sampling because temperature has a more significant effect on the lines studied here. Typical values of $\log_{10} g$ for A-type supergiants were estimated from Venn (1995) and Verdugo et al. (1999). Dufton et al. (2000) derive $\log_{10} g \approx 2.3$ for two B5 Iab stars, so $\log_{10} g = 2.5$ was taken as an upper limit for the hotter models. For the F and G spectral types considered here, Luck et al. (1997) find values over a range of $\log_{10} g = 0.0\text{--}1.0$, so spectra were synthesized for our coolest models using $\log_{10} g = 0.5$. The grid sampling is shown in Figure 6.

5.3 Abundances

For our calculations we have adopted a species-independent SMC metallicity based on the median differential abundances found by Venn (1999) for SMC A supergiants, i.e., $[X] = -0.76$ ($Z_{\text{SMC}} = 0.17Z_{\odot}$), where

$$[X] = \log_{10} \epsilon(X_{\text{SMC}}) - \log_{10} \epsilon(X_{\text{Gal}})$$

for species *X*, and

$$\log_{10} \epsilon(X) = \log_{10} (n(X)/n(\text{H})) + 12.$$

The adopted metallicity is broadly consistent with other recently published values for O and B-type stars (Haser et al. 1998, Dufton et al. 2000, Rolleston et al. 2003), F and K-type supergiants (Hill 1999) and Cepheids (Luck et al. 1997).

The metal abundances enter the modelling at two stages:

- In ATLAS, for the model-atmosphere calculation, Z_{Atlas} ;
- In SYNPEC, for the spectral-synthesis calculation, Z_{Syn} .

² <http://tlusty.gsfc.nasa.gov/> at the time of writing.

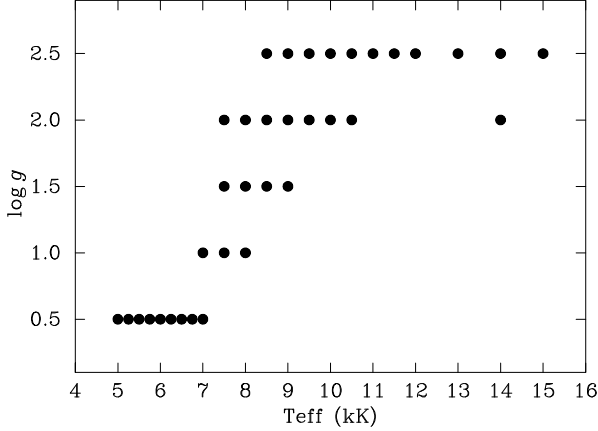


Figure 6. Grid of Kurucz models used to investigate the temperature scale of BAF-type SMC supergiants. The model atmospheres used were selected with consideration to expected typical values, though the coverage of the CCP7 grid is a limiting factor (*e.g.*, with the exception of $T_{\text{eff}} = 14\text{kK}$, the absence of $\log_{10} g = 2.0$ at higher temperatures).

Although there are no CCP7 ATLAS models specific to $[X] = -0.76$, grids at $[X] = -0.5$ and -1.0 (*i.e.* $Z_{\text{Atlas}} = 0.32Z_{\odot}$ and $0.10Z_{\odot}$) span our adopted metallicity. Since the dominant effect of metallicity in the computed spectra arises through the spectrum synthesis, not the atmospheric structures, we can use these ATLAS models for our purposes. We adopted the $0.32Z_{\odot}$ structure models, with $0.17Z_{\odot}$ for the spectral synthesis.

[The insensitivity of computed spectra to model structure is illustrated in Figure 7, which shows model profiles for $Z_{\text{Atlas}} = Z_{\odot}, 0.32Z_{\odot}$, and $0.10Z_{\odot}$ at $T_{\text{eff}} = 9000\text{K}$, $\log_{10} g = 1.5$, $Z_{\text{SSyn}} = 0.10Z_{\odot}$. When degraded to 2dF resolution, the resulting spectra are practically indistinguishable; the model-atmosphere structures calculated with different metallicities lead to essentially the same result, provided that the abundance is held constant in the spectrum synthesis. Similar results are obtained at $T_{\text{eff}} = 6000\text{K}$, $\log_{10} g = 0.5$, as shown in Figure 8, where the largest differences in rectified intensity are of order 2–3% – less than the uncertainties in the observed 2dF spectra.

These results are underpinned by inspection of the temperature profiles of the structure models. The profiles of the 9000K models, shown in Figure 9, are nearly identical for all three metallicities. The same is true of the 6000K models, shown in Figure 10. Only at large depths is the solar-abundance model significantly offset, but, as shown in Figure 8, the effect is small in terms of the emergent spectra.]

5.4 Spectral-type–temperature calibration

After rectification and smoothing, the synthetic spectra were assigned ‘high-resolution’ spectral types, using the criteria described in Section 4. Temperatures were then interpolated to the coarser grid of spectral types in Table 3. Galactic (solar) results were obtained by using the same procedures, to provide a directly comparable reference, and as a check on our methods. The calibrations are given in Table 5, and directly demonstrate the effect of SMC metallicity: at the

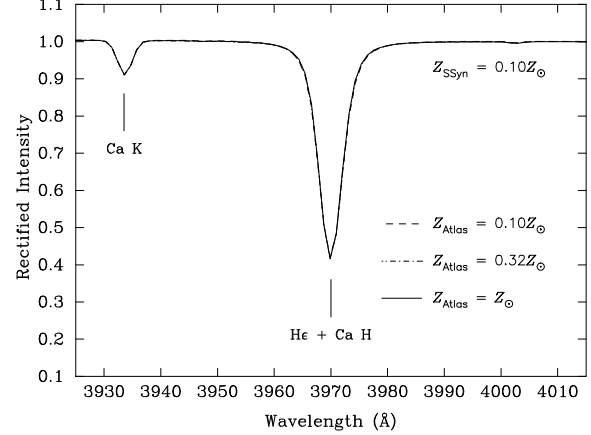


Figure 7. Model spectra for the Ca *K* region ($T_{\text{eff}} = 9000\text{K}$, $\log_{10} g = 1.5$), degraded to the resolution of the 2dF data. The metal abundances used in the spectral synthesis are $0.10Z_{\odot}$ in all cases; the abundances in the model atmospheres are solar, $0.32Z_{\odot}$, and $0.10Z_{\odot}$. The resulting spectra are essentially identical.

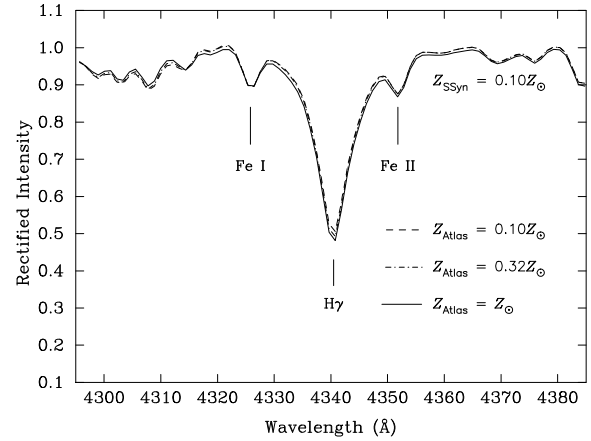


Figure 8. Model spectra of the H γ region ($T_{\text{eff}} = 6000\text{K}$, $\log_{10} g = 0.5$), degraded to the resolution of the 2dF data; abundances are as in Figure 7. The resulting spectra are again very similar.

same morphological spectral type, SMC stars are systematically cooler than Galactic counterparts, by up to $\sim 10\%$ at late A.

The explanation for this temperature offset is straightforward. The primary classification criterion used here involves the calcium and Balmer spectral lines. For sub-solar metallicity, the effective temperature has to be lower in order to increase the Ca *K* line strength to that required to satisfy the *K*/He criterion established from Galactic standards. This point is illustrated in Figure 11, using models at constant temperature but decreasing Z . (It may be noted that decreased metallicity also reduces the Balmer-line strength, because the pressure is reduced; but this is a much smaller effect than the direct impact on metal-line strengths.)

Given this interpretation, one might question whether the cooler SMC A-star temperatures highlighted here are simply a consequence of the particular classification criterion adopted. However, our temperature calibrations are in

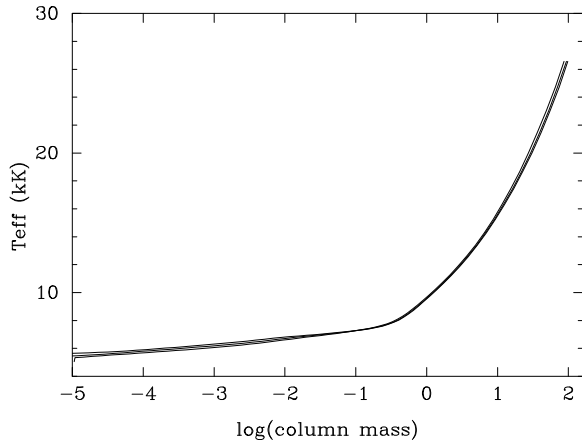


Figure 9. Atmospheric temperature profiles at $T_{\text{eff}} = 9000\text{K}$, $\log_{10} g = 1.5$. Models shown have $Z_{\text{Atlas}} = Z_{\odot}$, $0.32Z_{\odot}$ and $0.10Z_{\odot}$, and are essentially identical.

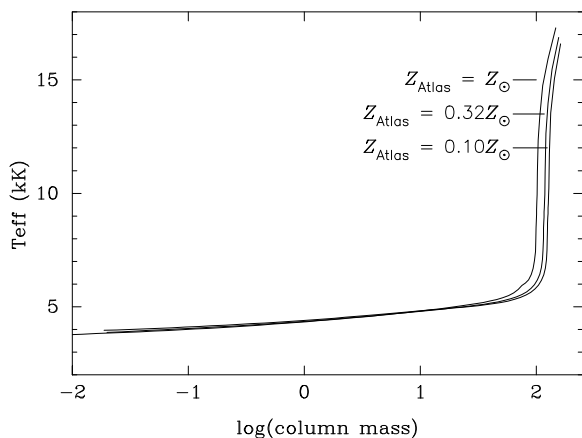


Figure 10. Atmospheric temperature profiles at $T_{\text{eff}} = 6000\text{K}$, $\log_{10} g = 0.5$. Models shown have $Z_{\text{Atlas}} = Z_{\odot}$, $0.32Z_{\odot}$ and $0.10Z_{\odot}$. The models differ only at large depths (see Section 5.3 for details).

excellent agreement with both the detailed analyses of individual Galactic stars given by Venn (1995), and with her results for early-A SMC supergiants (Venn 1999), which are based largely on the Mg^0/Mg^+ ionization balance. Nonetheless, there are differences in philosophy; for example, Venn (1999) obtained $T_{\text{eff}} = 7900\text{K}$ (and $\log_{10} g = 0.9$) for AV 442, and on that basis reclassified the star from A3 to A7, implicitly adopting a metallicity-independent relationship between spectral type and temperature. Our approach is to adopt spectral types consistently based solely on spectral morphology, but to accept a metallicity-dependent relationship between spectral type and physical parameters. That is, we would retain the A3 classification for AV 442, but would assign $T_{\text{eff}} = 8000\text{K}$ (Table 5). Three stars in Venn’s SMC sample appear to have temperatures that are inconsistent with those in Table 5 given their spectral types, namely AV 136 (Sk 54, A0 Ia), 478 (Sk 154, A0 Ib) and 213 (Sk 75, A2 Iab). These discrepancies appear to largely be a result of different published classifications, e.g. Venn’s temperatures are consistent with the spectral types of Humphreys et al.

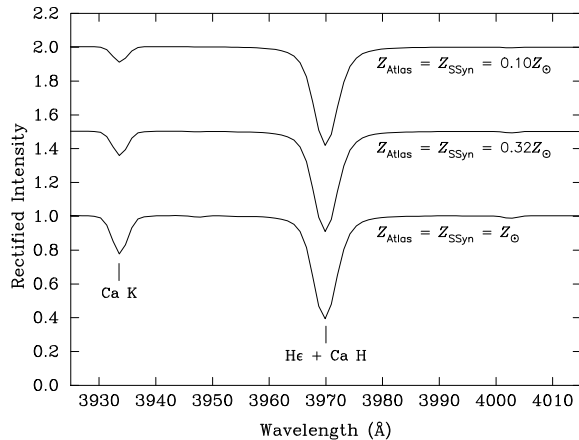


Figure 11. Model spectra for the Ca K region ($T_{\text{eff}} = 9000\text{K}$, $\log_{10} g = 1.5$), degraded to the resolution of the 2dF data. The metal abundances used in the spectral synthesis are identical to those used in the model-atmosphere calculations and are as shown.

Table 5. Solar-abundance and SMC temperature calibrations from the current work.

Type	Solar	SMC
B8	13000	12000
B9	10750	10500
A0	9750	9500
A2	9000	8500
A3	8500	8000
A5	8250	7750
A7	8000	7250
F0	7500	6750
F5	6250	5875
F8	6000	5750
G0	5875	5625
G2	5750	5500
G5	5500	5250

(1991) who gave classifications for AV 478 (A5 Iab) and AV 213 (A2–3 I).

Figure 12 compares the solar-abundance temperature scale derived here with those compiled by Schmidt-Kaler (1982) and by Humphreys & McElroy (1984). The main differences are at the very earliest and latest types considered here. The higher values we find for the late B-types are consistent with newer calibrations (e.g., Crowther 1998), so this is not a cause for concern. The differences in the later types, notably F5, could be attributable to the difficulties of classification in this region or to refinements in the model atmosphere codes (for example, the inclusion of molecular lines).

For simplicity we assumed a single relative abundance for all metallic species (i.e. $0.17Z_{\odot}$); however, detailed analyses such as those of Venn (1999) find a spread of abundances for different species. Venn specifically highlighted the relative underabundance of the alpha elements, including calcium (in contrast to the SMC H II region results from Russell & Dopita (1992) which found no calcium underabundance). To investigate the significance of adopting a

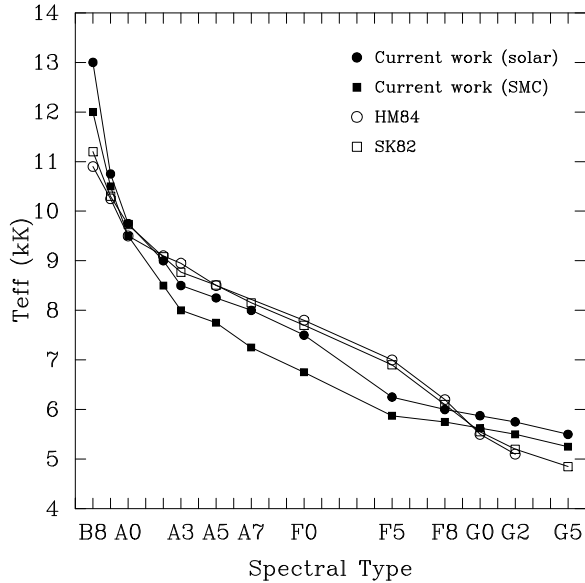


Figure 12. Solar and SMC temperature calibrations compared with those of Humphreys & McElroy (1984) and Schmidt-Kaler (1982). The differences for later spectral types between the published calibrations and our solar values, notably at F5, are likely attributable to difficulties of classification in this region and to refinements in the model atmospheres codes used here.

lower calcium abundance, model spectra ($Z = 0.10Z_{\odot}$) were calculated for 7500, 8000 and 8500 K, the domain in which the K line is most sensitive to temperature and abundance effects. Such a reduction enhances the temperature effect described here, but the change is very small compared to that between Galactic and ‘SMC’ abundances.

5.5 Luminosity implications

The present discussion of the relationship between temperature and spectral type in the reduced-metallicity environment of the SMC has immediate implications for the criteria used to allocate luminosity classes. At given spectral type, the temperature of an A-type SMC star is lower than its Galactic counterpart; as a consequence, the $H\gamma$ equivalent width will be different in the SMC star. For example, Figure 13 shows the model $H\gamma$ line for *i.e.* $T_{\text{eff}} = 9000\text{K}$, $Z = Z_{\odot}$ and $T_{\text{eff}} = 8500\text{K}$, $Z = 0.17Z_{\odot}$ (at $\log_{10} g = 2.0$), corresponding to Galactic and SMC A2 spectra, respectively; the $H\gamma$ equivalent width is some 30% larger in the SMC case. This is not (directly) a metallicity effect, as the $H\gamma$ lines for Galactic and SMC metallicities are essentially identical at fixed temperature.

Table 6 summarizes the differences in $H\gamma$ equivalent widths for stars of spectral types B8–A7 (averaged over $\log_{10} g$ at a given temperature). In general, equivalent widths are ~ 10 – 30% larger in the synthetic SMC spectra than in Galactic models at the same spectral type (but *not* the same temperature). Note that the equivalent widths are larger in *all* of the SMC spectra; in contrast to A-type dwarfs where the equivalent width of the Balmer lines reaches a maximum around A0/A2, the maximum for supergiants occurs

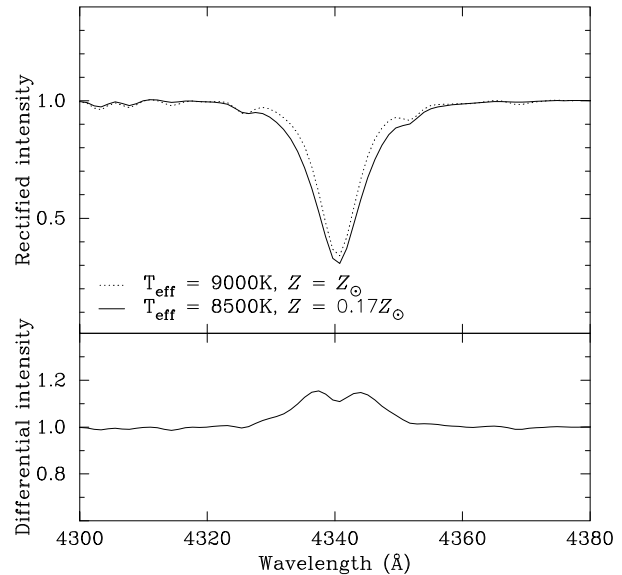


Figure 13. Model $H\gamma$ spectra at spectral type A2, for temperatures and metallicities appropriate for Galactic and SMC supergiants (with $\log_{10} g = 2.0$). The differential intensity plot in the lower panel emphasises of the difference in line strengths.

Table 6. Ratio of $H\gamma$ equivalent widths for Galactic and SMC model spectra corresponding to the same morphological types. The differences arise because of the lower temperatures of the SMC models at a given type, which, in the B8–A7 range results in increased equivalent widths.

Type	$H\gamma_{\text{SMC}} / H\gamma_{\text{Gal.}}$
B8	1.19
B9	1.08
A0	1.10
A2	1.29
A3	1.38
A5	1.27
A7	1.61

at a much later type (e.g. Hutchings 1966) resulting in a positive effect throughout the spectral types in Table 13. The clear implication is that if luminosity classifications are allocated from Galactic calibrations, the intrinsic brightness of a star with a given classification cannot be assumed to be universal.

6 DISCUSSION

Our work has demonstrated that accurate A-supergiant temperatures require knowledge of the metallicity of a system (and vice versa). This effect has important ramifications for studies of extragalactic A-type supergiants. For example, from comparison with template Galactic spectra, Bresolin et al. (2001) assign a spectral type of A1 Ia to a star in NGC 3621 (a spiral galaxy at a distance of 6.7 Mpc).

From the spectral type they estimate a temperature ($9000\text{K} \pm 400$) and then use Kurucz model atmospheres and the line formation calculations of Pryzbilla (2002) to find the chemical composition which best matches the observations; their final model has a chemical composition comparable to that of the Large Magellanic Cloud. The source of their temperature estimate is not given and unfortunately their spectra do not extend blueward to the Ca *K* line (their Figure 2). If the temperature were from Galactic analyses then the lower metallicity model would fail to reproduce the observed *K*-line intensity, requiring a reduction in the model temperature, leading to a different abundance determination; i.e. some degree of iteration is required.

Similar complications arise for the study of NGC 300 by Bresolin et al. (2002). Detailed atmospheric parameters were given for two supergiants, adopting temperatures from Humphreys & McElroy (1984) on the basis of their spectral types. The metallicity of their star ‘A-8’ (B9–A0 Ia) star is equivalent to that of the SMC, with $[X] = -0.7 \pm 0.2$. In light of the temperature effect described here, the uncertainty in such abundance determinations will be larger than ± 0.2 dex; even moderate changes of temperature can have a significant impact on the derived abundances (e.g. Venn 1999, Table 3).

The results presented here also have implications for the ‘flux-weighted gravity-luminosity relationship’ (FGLR) proposed by Kudritzki et al. (2003). They argue that for a given effective temperature (in their illustrative cases, assumed from the spectral type) the higher-order Balmer lines ($H\gamma$ through to $H11$) can be used to determine the gravity of distant A-type supergiants accurately. After calibration, the FGLR can in principle be used to determine the bolometric magnitude of a given star, hence the distance. Such a relationship is an attractive proposition for extragalactic distance determinations, especially since the atmospheric modelling only relies on the hydrogen lines which are thought to be well understood. However, in the context of the current work, consider the case of an A2 type supergiant, for which Kudritzki et al. (2003) adopt $T_{\text{eff}} = 9000\text{K}$. Such a temperature agrees with our solar-abundance temperature in Table 5; however, at SMC metallicity $T_{\text{eff}} = 8500\text{K}$ would be more appropriate. Herein lies a complication for the FGLR. The $H\gamma$ profile for a solar-abundance model with $T_{\text{eff}} = 9000\text{K}$ and $\log_{10} g = 2.0$ is similar to that for an SMC-abundance $T_{\text{eff}} = 8500\text{K}$, $\log_{10} g = 1.5$ model (Figure 14); the difference in M_{bol} from the FGLR from these two models is 1.7^m . With a finer sampling of gravity in the model grid the uncertainty in $\log_{10} g$ need not be as extreme as 0.5; nonetheless, the estimate of 0.05 by Kudritzki et al. must be considered rather optimistic. Disentangling the effects of temperature and metallicity in A-supergiants is non-trivial, impacting on their potential for use as extragalactic distance indicators.

7 CONCLUSION

We have observed a large number of A (and some later-type) supergiants as part of our 2dF survey of the SMC. To facilitate an accurate application of the MK process to our digital data, Galactic standards have been observed to provide a simple but quantitative temperature-classification scheme; the 2dF spectra have been classified within that scheme. A

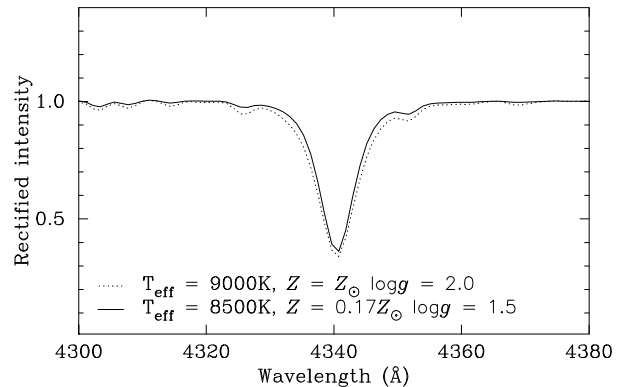


Figure 14. Model $H\gamma$ spectra at spectral type A2, for temperatures and metallicities appropriate for Galactic and SMC supergiants but with different gravities, $\log_{10} g = 2.0$ and 1.5 respectively.

direct result of classification based purely on morphological criteria is that, because the primary criterion involves both metallic and Balmer lines, the temperature of an SMC A-type supergiant is ~ 5 – 10% cooler than its Galactic counterpart. One of the main implications of this effect is that Galactic temperature calibrations should not necessarily be used when determining fundamental parameters and abundances for extragalactic A-supergiants.

In addition to its significance for individual stars, this result has implications for population-synthesis studies. Such investigations typically involve generating a synthetic population from stellar-evolution models, and then transforming the model predictions to observational parameter space. This transformation necessarily always involves a calibration between observed and modelled parameters; if the calibration is based on Galactic stars, then significant errors can be introduced into the interpretation of low-metallicity environments, even when the synthetic population is generated using stellar-evolution models at the appropriate metallicity.

8 ACKNOWLEDGEMENTS

CJE was funded by PPARC during the course of this work. IDH is a Fresia Jolligoode Fellow, and acknowledges support from SWIMBO. We thank Ivan Hubeny and the CCP7 project for assistance with the model-atmosphere work, and the staffs of the Anglo-Australian Observatory and of the Isaac Newton Group for support at the telescopes. We are grateful to Kim Venn and Nolan Walborn for their detailed comments on the manuscript. This paper is based in part on data obtained with the Isaac Newton and William Herschel Telescopes, operated on the island of La Palma by the Isaac Newton Group in the Spanish Observatorio del Roque de los Muchachos of the Instituto de Astrofísica de Canarias, and with the Anglo-Australian Telescope.

REFERENCES

Abt H. A., 1981, *ApJS*, 45, 437

- Abt H. A., 1985, *ApJS*, 59, 95
 Abt H. A., Morrell N. I., 1995, *ApJS*, 99, 135
 Azzopardi M., 1987, *A&AS*, 69, 421
 Balona L., Crampton D., 1974, *MNRAS*, 166, 203
 Bresolin F., Gieren W., Kudritzki R.-P., Pietrzyński G., Przybilla N., 2002, *ApJ*, 567, 277
 Bresolin F., Kudritzki R.-P., Mendez R. H., Przybilla N., 2001, *ApJ*, 548, 159L
 Brotherton M. S., van Breugel W., Stanford S. A., Smith R. J., Boyle B. J., Miller L., Shanks T., Croom S. M., Filippenko A. V., 1999, *ApJ*, 520, L87
 Cannon A. J., Pickering E. C., 1918–1924, *Annals Harvard Obs.*, 91–99
 Cowley A., Cowley C., Jaschek M., Jaschek C., 1969, *AJ*, 74, 375
 Crowther P. A., 1998, in Bedding T. R., Booth A. J., Davis J., eds, *Fundamental Stellar Properties: The Interaction between Observation and Theory*, IAU Symposium No. 189 Kluwer, Dordrecht, p. 137
 Dufton P. L., McErlean N. D., Lennon D. J., Ryans R. S. I., 2000, *A&A*, 353, 311
 Evans C. J., Howarth I. D., Irwin M. J., 2003, *MNRAS*, submitted
 Fitzgerald M. P., 1970, *A&A*, 4, 234
 Gray R. O., Garrison R. F., 1987, *ApJS*, 65, 581
 Gray R. O., Garrison R. F., 1989, *ApJS*, 70, 623
 Gray R. O., Napier M. G., Winkler L. I., 2001, *AJ*, 121, 2148
 Hartmann J., 1904, *ApJ*, 19, 268
 Haser S. M., Pauldrach A. W. A., Lennon D. J., Kudritzki R.-P., Lennon M., Puls J., Voels S. A., 1998, *A&A*, 330, 285
 Hendry E. M., 1981, *AJ*, 86, 1540
 Hill V., 1999, *A&A*, 345, 430
 Humphreys R. M., 1978, *ApJS*, 38, 309
 Humphreys R. M., 1983, *ApJ*, 265, 176
 Humphreys R. M., Kudritzki R.-P., Groth H. G., 1991, *A&A*, 245, 593
 Humphreys R. M., McElroy D. B., 1984, *ApJ*, 284, 565
 Hutchings J. B., 1966, *MNRAS*, 132, 433
 Jaschek C., Jaschek M., 1990, *The Classification of Stars*. Cambridge University Press, Cambridge
 Kudritzki R.-P., Bresolin F., Przybilla N., 2003, *ApJ*, 582, 83L
 Kurucz R. L., 1991, in Crivellari L., Hubeny I., Hummer D. G., eds, *Stellar Atmospheres: Beyond Classical Models* Kluwer, Dordrecht, p. 441
 Lennon D. J., 1997, *A&A*, 317, 871
 Lewis I. J., Cannon R. D., Taylor K., Glazebrook K., Waller L. G., Whittard J. D., Wilcox J. K., Willis K. C., 2002, *MNRAS*, 333, 279
 Luck R. E., Moffett T. J., Barnes T. G., Gieren W. P., 1997, *AJ*, 115, 605
 Maeder A., Grebel E. K., Mermilliod J. C., 1999, *A&A*, 346, 459
 Maury A. C., 1897, *Annals Harvard Obs.*, 28, 1
 McAlister H. A., 1979, *PASP*, 90, 288
 McCarthy J. K., Lennon D. J., Venn K. A., Kudritzki R.-P., Puls J., Najarro F., 1995, *ApJ*, 455, L135
 Mermilliod J.-C., Mermilliod M., Hauck B., 1997, *A&AS*, 124, 349
 Morgan W. W., Keenan P. C., 1973, *ARA&A*, 11, 29
 Morgan W. W., 1937, *ApJ*, 85, 380
 Morgan W. W., Code A. D., Whitford A. E., 1955, *ApJS*, 2, 41
 Morgan W. W., Harris D. L., Johnson H. L., 1953, *ApJ*, 118, 92
 Morgan W. W., Keenan P. C., Kellman E., 1943, *An atlas of stellar spectra*. Chicago Univ. Press
 Morgan W. W., Roman N. G., 1950, *ApJ*, 112, 362
 Pickering E. C., 1890, *Annals Harvard Obs.*, 27, 1
 Przybilla N., 2002, PhD thesis, Univ. of Munich
 Rolleston W. R. J., Venn K. A., Tolstoy E., Dufton P. L., 2003, *A&A*, 400, 21
 Russell S. C., Dopita M. A., 1992, *ApJ*, 384, 508
 Schmidt-Kaler T., 1982, in Schaifers K., Voigt H. H., eds, *Landolt-Börnstein, Group VI, Vol 2b Springer-Verlag*, p. 1
 Slettebak A., 1954, 1954, 119, 146
 Venn K. A., 1995, *ApJS*, 99, 659
 Venn K. A., 1999, *ApJ*, 518, 405
 Venn K. A., McCarthy J. K., Lennon D. J., Przybilla N., Kudritzki R.-P., Lemke M., 2000, *ApJ*, 541, 610
 Verdugo E., Talavera A., Gómez de Castro A. I., 1999, *A&A*, 346, 819
 Walborn N. R., 1979, in McCarthy M. F., Philip A. G. D., Coyne G. V., eds, *Spectral Classification of the Future*, IAU Coll. 47 Vatican Observatory, p. 337
 Yamashita Y., Nariai K., Norimoto Y., 1977, *An atlas of representative stellar spectra*. Univ. of Tokyo Press